



Published in final edited form as:

J Magn Reson. 2010 July ; 205(1): 63–68. doi:10.1016/j.jmr.2010.04.001.

Susceptibility-matched plugs for microcoil NMR probes

Ravi Kc, Yashas N. Gowda, Danijel Djukovic, Ian D Henry, Gregory H J Park, and Daniel Raftery

Department of Chemistry, Purdue University, West Lafayette, IN 47907

Abstract

For mass limited samples, the residual sample volume outside the detection coil is an important concern, as is good base line resolution. Here, we present the construction and evaluation of magnetic susceptibility-matched plugs for microcoil NMR sample cells which address these issues. Mixed-epoxy glue and ultem tube plugs that have susceptibility values close to those of perfluorocarbon FC-43 (fluorinert) and copper were used in small volume (0.5 to 2 μL) and larger volume (15 to 20 μL) thin glass capillary sample cells. Using these plugs, the sample volume efficiency (i.e. ratio of active volume to total sample volume in the microcoil NMR cell) was improved by 6 to 12 fold without sensitivity and resolution trade-offs. Comparison with laser etched or heat etched microcoil sample cells is provided. The approaches described are potentially useful in metabolomics for biomarkers detection in mass limited biological samples.

Keywords

susceptibility-matched plug; ^1H NMR; microcoil; metabolomics; SNR enhancement; volume efficiency

Introduction

Nuclear magnetic resonance (NMR) spectroscopy is a premier analytical method for molecular structure determination, and is widely used in chemical and pharmaceutical research. As such, NMR is increasingly used for the analysis of complex samples such as biofluids.¹ Yet the sensitivity of NMR is sometimes limiting, and therefore a variety of sensitivity enhancement techniques^{2–6} have been introduced. Among these methods, microcoil NMR has been shown to improve mass-sensitivity, S_m (SNR per micromole) dramatically, which is achieved by the use of smaller diameter detection coils.⁷

Microcoils that utilize a solenoidal geometry with multiple coil-turns enhance the coil sensitivity compared to the standard Helmholtz coil geometry⁸ used in NMR probes. However, several factors affect the spectral resolution that is dependent on the static magnetic field inhomogeneity inside the coil volume. Field inhomogeneity can arise from magnetic susceptibility differences between the coil and surrounding air, coil winding pitch and coil turns, sample length and shape, the ratio of coil length to its diameter and even the thickness

© 2010 Elsevier Inc. All rights reserved

*Author to whom correspondence should be addressed: Dr. Daniel Raftery Professor of Chemistry Purdue University Department of Chemistry 560 Oval Dr. West Lafayette, IN 47907 Office: (765) 494-6070 FAX: (765) 494-0239 raftery@purdue.edu.

Publisher's Disclaimer: This is a PDF file of an unedited manuscript that has been accepted for publication. As a service to our customers we are providing this early version of the manuscript. The manuscript will undergo copyediting, typesetting, and review of the resulting proof before it is published in its final citable form. Please note that during the production process errors may be discovered which could affect the content, and all legal disclaimers that apply to the journal pertain.

of the sample cell holder.^{9–14} The susceptibility mismatch between the copper coil and the sample can be dramatically reduced by immersing the solenoidal coil/sample system in a perfluorocarbon FC-43 (fluorinert) fluid that has a close susceptibility match to copper.⁷ Alternatively, zero-susceptibility wire can be used to avoid the usage of susceptibility matching fluid.^{14–16} While a variable pitch¹¹ solenoidal coil is preferred, a shorter solenoid with a greater number of turns¹³ is best suited for obtaining a homogenous RF magnetic field. On the other hand, the thickness of the sample cell holder needs to be optimized to obtain optimum sensitivity by increasing the fill factor^{17,18} while avoiding resolution degradation due to the proximity of the sample and coil in thinner sample holder walls.¹⁹

With all the above criteria fulfilled, good resolution in microcoil NMR can be achieved (below 1 Hz at FWHM, full width of half-maximum).^{7,17,18,20} Additionally, the baseline resolution has to be equally considered if microcoil probes are to be utilized for analyzing complex bio-samples. Fuks *et al.*¹⁰ elucidated that, in order to reduce end-effects from the perturbing magnetic field and thereby achieve a nearly constant field at the center of the tube, the lengths of the coil and glass tube should be at least 1–2 fold larger than their diameters. For longer microcoil glass tubes, the baseline resolution at 0.55% / 0.11% peak height can be reduced below 20/30 Hz. This constraint on the sample tube typically leads to the requirement for larger sample volumes needed to fill not only long residual sample tube volume across each end of the small coil, but also input and output flow transfer lines. Thus, the volume efficiency defined as the ratio of active volume to total sample volume degrades. For example, if the detection volume is 1 μL , the total sample volume might be 50–60 μL or even 100–150 μL for a 20 μL detection volume, depending on the inner diameter and length of sample tube and transfer lines.^{17,18,21} Further, the diameter of the transfer lines has to be optimized to provide easy flow of viscous samples. Larger volume requirements often result in the dilution of mass-limited samples, thus reduced sample sensitivity. Etching techniques^{17,18,22,23} can be used to create a “bubble” sample cell that increases the fill factor and lowers the sample volume in the regions outside the active detection volume. However, this approach often leads to thicker glass wall regions at each end of the coil, which changes the volume susceptibility difference between the sample and the glass-wall^{17,18} and creates wider baselines. Alternatively, the sample can be sandwiched between plugs of immiscible fluorocarbon fluid FC-43^{21,24,25} which reduces the residual sample volumes inside the probe without degrading baseline resolution. However, miscibility of the analytes in the FC-43 fluid must be considered before using sandwiching fluid with the sample. Also, if sample recovery (such as for MS analysis) is required, this is more difficult.

Another approach, which we introduce below, is to incorporate solvent susceptibility-matched solid plugs into the horizontal microcoil sample flow-tube. Solvent-susceptibility matched plugs are often used in conjunction with standard NMR tubes and are inserted in the sample tube to remove susceptibility differences at the air-sample or glass-sample interfaces that is not parallel to B_0 . Susceptibility plugs also reduce the required sample amount for NMR analysis by up to 80% (Doty Scientific, Columbia, SC). Using a similar approach, we demonstrate the use of solid ultem and dried epoxy-glue plugs in larger (greater than 15–20 μL or 2 mm ID sample cell tube) and small volume (less than a few μL or 1 mm ID sample cell tube) microcoil cells, respectively. The plugs have close magnetic-susceptibility values to surrounding fluorinert FC-43 and copper in the coil. The technique is simple and easy to implement allowing the designer to adjust the plug length to optimize baseline resolution. This approach provides sample volume reductions by 6–12 fold without compromising resolution or sensitivity as compared to the microcoil cells without plugs. Performance of the proposed technique is shown in terms of volume efficiency, resolution, line shape and sensitivity, as well as high resolution 1D and 2D spectra. The resolution performance using susceptibility matched plugs is also compared to our previous probes^{17,18} that used etching techniques to reduce sample volume and to improve fill factor. Potential applications and on-going work in the study

and structural identification of metabolites in human plasma/serum and urine samples using this technique are discussed.

Methods

Sample Cell Construction

Plug types and the corresponding sample tube sizes were chosen based on ease of implementation, commercial availability and practicality. For example, ultem plugs were used in larger volume capillary glass cells (larger ID ≥ 2 mm) while dried epoxy-glue plugs were used for smaller volume capillary glass cells (smaller ID ≤ 1 mm ID) since it was much easier to make a plug by flowing/drying glue in small ID tubes than to custom machine solid ultem plugs with diameters below 1 mm. Ultem and mixed-epoxy were used as plugs for their volume magnetic susceptibility values (χ_v , cgs) that are close to those for susceptibility matching fluid fluorinert FC-43 and RF coil copper wire ($\chi_v = -0.71 \times 10^{-6}$ for ultem; $= -0.699 \times 10^{-6}$ for mixed epoxy; FC-43 $= -0.70 \times 10^{-6}$, and Cu wire $= -0.78 \times 10^{-6}$).^{26–29}

As shown in the schematic drawing in Figure 1A, for the larger volume cell, two 1 cm long thick wall tubes (2.36 mm. OD, ~ 0.8 mm ID; CPI Intl., Santa Rosa, CA) were cut. Two pieces of 1 cm long flexible Teflon tubing (0.76 mm OD, 0.300 mm ID; Cole-Parmer, Vernon Hills, IL) were inserted and glued into each ultem plug with a little epoxy (Devcon, Danvers, MA). Flexible teflon tubing was used to make a joint between the ultem plug and input/output transfer lines. Each 55 cm long fused silica transfer line (360 μ m OD, 70 μ m ID; Polymicro Technologies, Phoenix, AZ) was glued to a 1 cm piece of teflon tubing using epoxy. Finally, the open end of each ultem plug (with the glued teflon tubing and fused silica capillary at its other end) was inserted and epoxied into a 2 cm long thin glass capillary (2.8 mm OD, 2.423 mm ID; Friedrich & Dimmock, Millville, NJ), leaving a 5 mm long detection region at the center. A variable pitch RF coil was manually wound with four turns of round copper wire (150 μ m OD, polyimide-coated; California Fine Wire, Grover Beach, CA) at the center of the above sample glass capillary to produce a 4.3 mm long coil that covered the 20 μ L detection volume with less than 4 μ L residual volume outside the coil ends.

Smaller sample cells were constructed from 1 mm OD and 1.43 mm OD thin glass capillaries (Friedrich & Dimmock, Millville, NJ), resulting in 500 nL and 2 μ L detection volumes, respectively. As shown in the schematic drawing in Figure 2, two 1 cm long fused silica capillaries (360 μ m OD, 70 μ m ID; Polymicro Technologies, Phoenix, AZ) were inserted and glued to each end of the thin glass capillaries using epoxy. To control the length of the glue plug inside the cells precisely, partially air-filled syringes were connected to each end of the fused silica capillaries (Fig. 2A). The syringes were pulled in or out either to flow the glue into the cells or to prevent the overflow of the glue into the detection volume. Plug lengths were adjusted by leaving 3 or 4 mm central detection regions for the 1 mm OD and 1.43 mm OD cells, respectively. A variable pitch RF coil was manually wound with five turns of 150 μ m OD round copper wire (California Fine Wire, Grover Beach, CA) at the center of each small volume sample cell. The RF coils had lengths of approximately 2.55 mm and 2.32 mm, resulting in detection volumes of 500 nL (< 0.5 μ L residual volume) and 2 μ L (< 1.5 μ L residual volume), respectively. Each end of the fused silica capillaries were connected to 1 cm long flexible Teflon tubing which was again connected to 55 cm fused silica transfer lines (not shown in Fig. 2).

Both the larger volume and small volume coils were tuned and matched^{30,31} to a ^1H frequency of 300 MHz with two variable capacitors (0.1–9 pF, Voltronics, Denville, NJ), and one fixed-value capacitor (2.2 pF ATC, Huntington Station, NY) as shown in Fig. 2C. A 2-cm long, 0.181-in. OD, 50 Ω semi-rigid coaxial cable (Haverhill Manufacturing, Haverhill, MA) was used to connect each coil to its respective circuit elements. Each coil was immersed in

susceptibility matching fluid fluorinert FC-43. Other homogeneous field parameters for small and larger volume coils were kept constant including maintaining the ratio of coil-length to coil-diameter ≥ 1 , the ratio of sample-length to coil-length ≥ 1 , and the height (~1.8 cm) of each coil center from the base of the fluorinert holding container.

Sample Preparation

Isotopically-enriched D₂O (99.9%) was purchased from Cambridge Isotope (Andover, MA), Sucrose and threonine standards were purchased from Mallinckrodt Baker (Phillipsburg, NJ), and Sigma-Aldrich (St. Louis, MO) respectively. 1% v/v H₂O/D₂O, 40 mM solutions of sucrose and threonine in D₂O, as well as deproteinated human plasma samples were prepared. Each 40 mM standard solution was further mixed with one another to make nearly 20 mM concentrations in the final mixture. Standard human plasma samples were obtained from commercial sources. Plasma was pretreated for deproteination as described previously,³² except the final duplicate plasma samples were prepared in 40 μ L and 600 μ L of D₂O, to compare SNR enhancement between a microcoil probe utilizing susceptibility plugs and a 5 mm conventional probe (4-nucleus Nalorac, 300 MHz).

NMR Experiments

1D ¹H NMR experiments were performed using a Varian INOVA 300 MHz NMR spectrometer installed with VNMR 6.1 processing software. Prepared samples were injected into the probes using a 50 μ L Hamilton syringe (Hamilton, Reno, NV) and syringe adapter (VICI Valco, Houston, TX).

Each probe was manually shimmed to obtain the best line width and line shape. Raw signal to noise ratios (SNR) were calculated without any processing parameters such as zero-filling and apodization. For small diameter coils, the ¹H 90° pulse length was measured to be 2.4 μ s at 40 dB. For the larger diameter coil, the ¹H 90° pulse length was 6.2 μ s at 40 dB. A recycle delay time of 1.5 s was used for all the NMR experiments. A constant concentration sample of 1% v/v H₂O/D₂O was used to assess the resolution, line shape and SNR for the microcoil probes with susceptibility matched plugs. The performance of the coils was further tested by running 1D ¹H NMR and 2D COSY experiments for the standard glucose and threonine mixture. In addition, the applicability of the coils to analyze complex biological mixtures was assessed using 1D ¹H NMR of treated human plasma samples.

Results

For the most part, ¹H resolution and line shape results (see Fig. 3 and Table 1) were obtained with better than 1 Hz at FWHM and less than 30/40 Hz at 0.55% /0.11% peak heights. Figure 3 also includes the spectrum acquired in a small diameter (1.0 mm OD) capillary tube cell that was manually customized by grinding a 2.36 mm OD, ~0.8 mm ID Ultem tube (CPI Intl., Santa Rosa, CA) with a Dremel® (Racine, WI) hand tool. The Ultem cell was used to investigate if better resolution and line shape could be obtained by lowering the susceptibility differences around the sample region. Theoretically, the susceptibility difference values between ultem/mixed-epoxy is smaller than glass/mixed-epoxy. Although similar resolution was obtained, the line shape was better using the Ultem cell with epoxy plugs.

Table 1 shows a comparison of the results for different diameter coils with and without susceptibility matched plugs in terms of their volume efficiency, resolution and SNR. Using a susceptibility-matched plug, a nearly 6–12 fold improvement in volume efficiency can be achieved without significant loss in resolution and sensitivity for both the smaller and larger volume microcoils. The 20- μ L volume cell has similar resolution to that for the smaller coils, but has more than 5-fold better SNR for the constant concentration sample of H₂O/D₂O.

Additionally, in comparison to a standard 5 mm probe that requires 600 μL total sample volume, the 20 μL cell probe has a 30 μL total sample volume and therefore offers a volume efficiency enhancement of 20 fold (of course, the use of Doty susceptibility plugs and Shigemitsu tubes would reduce this enhancement factor).

Figure 4 shows highly resolved 1D ^1H spectra (36 scans) and 2D COSY (8 scans and 128 increments) of the two standard compound mixture – glucose and threonine, acquired in 20- μL ultem plug cell (2.8 mm OD). The figure also shows the spectrum for the deproteinated human plasma sample acquired with 36 scans in the same microcoil susceptibility plug probe (lower) in comparison to the commercial 5 mm probe (upper). Lower inset shows a highly resolved peak (~ 5.2 ppm) for the anomeric proton from α -glucose in plasma at the base of the solvent (~ 4.7 ppm). The raw SNR for this proton was 28.5:1, which is 9.5-fold higher than that for 5-mm probe for the same mass of analyte. Similar resolution and SNR enhancement (figure not included) was obtained in smaller coils with epoxy plugs.

Discussion

We demonstrate here that the use of small epoxy and Ultem plugs can be of high utility to improve the volume efficiency of microcoil probes. Volume efficiency is often a major concern in the analysis of mass limited samples. In this study, high volume efficiency without trade-offs in sensitivity and resolution was achieved by introducing susceptibility-matched plugs into the microcoil sample cells. Our previous probes that employed etching techniques to create ellipsoidal bubble detection cells^{17,18} yielded FWHM line widths of less than 1 Hz; however, the baseline resolution was poorer, with 0.55%/0.11% peak values of 80/120 Hz. Imprecise etching often resulted in relatively large bubble cells that increased the residual volume and lowered the volume efficiency. Incorporation of the susceptibility-matched plugs greatly alleviates these problems.

The flexibility of the proposed approach allows one to adjust the plug to increase or decrease the desired detection volume. Application of such probes can be envisioned in hyphenation with HPLC in which the potential issues, such as system dead volume, the imperfect match between HPLC elution and NMR detection volumes, sharp concentration gradients near the NMR coil, the equilibration time in moving the analyte from HPLC to NMR coil, and the sample diffusion from the flow cell can be minimized by eliminating residual volumes as much as possible.²¹ Another major application of the plugged microcoil probes is targeted towards analyzing mass limited metabolic samples and biofluids in which one can optimize the detection limit by taking maximum advantage of the available sample. Better sample volume efficiency provides the option of using increased sample concentration, and thus, decreased experiment time.

The raw SNR for the 20- μL solenoidal microcoil probe is approximately 5-fold less than observed in the 5 mm commercial probe. This value is less than what would be expected by simply comparing active volumes because the loss is mitigated by the solenoid geometry. When the sample can be concentrated, we find that the improved volume efficiency and other positive attributes of the plugged-microcoil approach yield an overall 8 to 10-fold enhancement in SNR based on the improved mass sensitivity. The experimental results (shown in Fig. 4C) yield values close to this rough calculation. While the ultem or epoxy plugs are not compatible with all organic solvents, this approach is highly useful for bio-fluid or other aqueous samples. Along with high mass-sensitivity, the enhanced SNR due to effective volume management of the susceptibility plug microcoil probe may provide a practical solution for the NMR analysis of a variety of precious samples. Currently, we are using susceptibility plug microcoil probes for the analysis and structural identification of low concentration metabolites in human plasma/serum and urine samples.

Acknowledgments

Financial support from the NIH (Grants 1R01GM085291-01 and 1P01AT004511-01) and invaluable suggestions from Dr. G. A. Nagana Gowda for this project are gratefully acknowledged.

References

1. Gowda GAN, Zhang SC, Gu HW, Asiago V, Shanaiah N, Raftery D. Metabolomics-based methods for early disease diagnostics. *Expert Review of Molecular Diagnostics* 2008;8(5):617–633. [PubMed: 18785810]
2. Ardenkjaer-Larsen JH, Fridlund B, Gram A, et al. Increase in signal-to-noise ratio of > 10,000 times in liquid-state NMR. *Proceedings of the National Academy of Sciences of the United States of America* 2003;100(18):10158–10163. [PubMed: 12930897]
3. Rugar D, Zuger O, Hoen S, Yannoni CS, Vieth HM, Kendrick RD. Force detection of Nuclear-Magnetic-Resonance. *Science* 1994;264(5165):1560–1563. [PubMed: 17769597]
4. Sakellariou D, Le Goff G, Jacquinet JF. High-resolution, high-sensitivity NMR of nanolitre anisotropic samples by coil spinning. *Nature* 2007;447(7145):694–697. [PubMed: 17554303]
5. Savukov IM, Lee SK, Romalis MV. Optical detection of liquid-state NMR. *Nature* 2006;442(7106):1021–1024. [PubMed: 16943834]
6. Styles P, Soffe NF, Scott CA, et al. A high-resolution NMR probe in which the coil and preamplifier are cooled with liquid helium. *Journal of Magnetic Resonance* 1984;60(3):397–404.
7. Olson DL, Peck TL, Webb AG, Magin RL, Sweedler JV. High-resolution microcoil H-1-NMR for mass-limited, nanoliter-volume samples. *Science* 1995;270(5244):1967–1970.
8. Olson DL, Norcross JA, O'Neil-Johnson M, et al. Microflow NMR: Concepts and capabilities. *Analytical Chemistry* 2004;76(10):2966–2974. [PubMed: 15144211]
9. Callaghan PT. Susceptibility-limited resolution in Nuclear-Magnetic-Resonance microscopy. *Journal of Magnetic Resonance* 1990;87(2):304–318.
10. Fuks LF, Huang FSC, Carter CM, Edelstein WA, Roemer PB. Susceptibility, lineshape, and shimming in high-resolution NMR. *Journal of Magnetic Resonance* 1992;100(2):229–242.
11. Idziak S, Haerlen U. Design and construction of a high homogeneity rf coil for solid-state multiple-pulse NMR. *Journal of Magnetic Resonance* 1982;50(2):281–288.
12. Levitt MH. Demagnetization field effects in two-dimensional solution NMR. *Concepts in Magnetic Resonance* 1996;8(2):77–103.
13. Peck TL, Magin RL, Lauterbur PC. Design and analysis of microcoils for NMR microscopy. *Journal of Magnetic Resonance Series B* 1995;108(2):114–124. [PubMed: 7648010]
14. Zelaya FO, Crozier S, Dodd S, McKenna R, Doddrell DM. Measurement and compensation of field inhomogeneities caused by differences in magnetic-susceptibility. *Journal of Magnetic Resonance Series A* 1995;115(1):131–136.
15. Soffe N, Boyd J, Leonard M. The construction of a high-resolution 750 MHz probehead. *Journal of Magnetic Resonance Series A* 1995;116(1):117–121.
16. Kc R, Henry ID, Park GHJ, Aghdasi A, Raftery D. New Solenoidal Microcoil NMR Probe using Zero-susceptibility Wire. *Concepts in Magnetic Resonance Part B-Magnetic Resonance Engineering* 2010;37B(1):13–19.
17. Henry ID, Park GHJ, Kc R, Tobias B, Raftery D. Design and construction of a microcoil NMR probe for the routine analysis of 20- μ L samples. *Concepts in Magnetic Resonance Part B-Magnetic Resonance Engineering* 2008;33B(1):1–8.
18. Kc R, Henry ID, Park GHJ, Raftery D. Design and construction of a versatile dual volume heteronuclear double resonance microcoil NMR probe. *Journal of Magnetic Resonance* 2009;197(2):186–192. [PubMed: 19138541]
19. Webb AG, Grant SC. Signal-to-noise and magnetic susceptibility trade-offs in solenoidal microcoils for NMR. *Journal of Magnetic Resonance Series B* 1996;113(1):83–87. [PubMed: 8888593]
20. Webb AG. Radiofrequency microcoils in magnetic resonance. *Progress in Nuclear Magnetic Resonance Spectroscopy* 1997;31:1–42.

21. Kautz RA, Goetzinger WK, Karger BL. High-throughput microcoil NMR of compound libraries using zero-dispersion segmented flow analysis. *Journal of Combinatorial Chemistry* 2005;7(1):14–20. [PubMed: 15638474]
22. Pusecker K, Schewitz J, Gfroerer P, Tseng LH, Albert K, Bayer E. On line coupling of capillary electrochromatography, capillary electrophoresis, and capillary HPLC with nuclear magnetic resonance spectroscopy. *Analytical Chemistry* 1998;70(15):3280–3285.
23. Zhang XF, Webb AG. Magnetic resonance microimaging and numerical simulations of velocity fields inside enlarged flow cells used for coupled NMR microseparations. *Analytical Chemistry* 2005;77(5):1338–1344. [PubMed: 15732916]
24. Behnia B, Webb AG. Limited-sample NMR using solenoidal microcoils perfluorocarbon plugs, and capillary spinning. *Analytical Chemistry* 1998;70(24):5326–5331. [PubMed: 9868921]
25. Lacey ME, Sweedler JV, Larive CK, Pipe AJ, Farrant RD. H-1 NMR characterization of the product from single solid-phase resin beads using capillary NMR flow probes. *Journal of Magnetic Resonance* 2001;153(2):215–222. [PubMed: 11740897]
26. Keyser PT, Jefferts SR. Magnetic-susceptibility of some material used for apparatus construction (at 295-K). *Review of Scientific Instruments* 1989;60(8):2711–2714.
27. Macnaughtan, MA. Multiple-coil NMR probes for high-throughput and difference spectroscopy [Ph. D. Thesis]. Purdue University; West Lafayette: 2003.
28. Lide, DR., editor. *CRC Handbook of Chemistry and Physics*. CRC Press; Boca Raton, FL: 2008–2009.
29. Specifications from Wilmad Co.; Buena, NJ: 2008.
30. Gadian DG, Robinson FNH. Radiofrequency losses in NMR experiments on electrically conducting samples. *Journal of Magnetic Resonance* (1969) 1979;34(2):449–455.
31. Murphy-Boesch J, Koretsky AP. An in Vivo NMR probe circuit for improved sensitivity. *Journal of Magnetic Resonance* (1969) 1983;54(3):526–532.
32. Ye T, Mo H, Shanaiah N, Gowda GAN, Zhang S, Raftery D. Chemoselective ¹⁵N Tag for Sensitive and High-Resolution Nuclear Magnetic Resonance Profiling of the Carboxyl-Containing Metabolome. *Analytical Chemistry* 2009;81(12):4882–4888. [PubMed: 19518144]

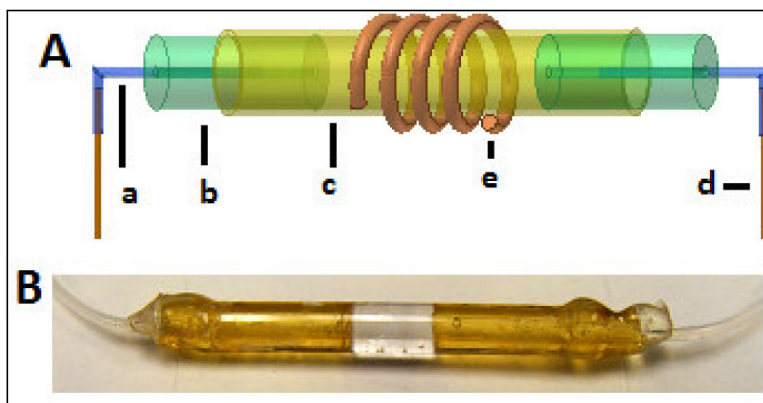


Fig. 1. **A** - Procedure for creating 20- μL detection sample cell with susceptibility-matching ultem plugs. Each insert consisted of a) 1 cm long, 300- μm ID tefton tubing; b) 1cm long, 2.36 mm. OD, ~0.8 mm ID ultem plug; c) 2.8 mm OD, 2.42 mm ID, 2 cm long glass capillary; and d) 55 cm long, 360 μm OD, 70 μm ID fused silica transfer line. The length of the ultem plugs inside a glass capillary is adjusted to cover slightly more than a desired active volume defined by a 4 turn copper wire (150 μm OD) coil (e). Total sample volumes of the cell and transfer lines are 24 μL and 4.5 μL (each), respectively compared to a 140 μL total volume without the ultem plugs. **B** - Actual sample cell with ultem plugs and tefton transfer line inserts.

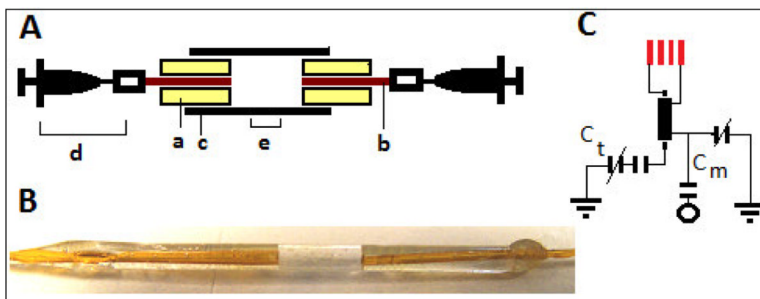


Fig. 2.

A: Procedure for creating a 500-nL to 2- μ L detection sample cells with susceptibility-matched epoxy plugs. Flow of (a) epoxy-mixture along the outside wall of (b) fused silica transfer lines (1 cm long, 360 μ m OD 70 μ m ID) inside each end of (c) thin glass capillary (2 cm long, 1 mm or 1.43 mm OD) is controlled with the suction of the (d) air-filled syringes fixed at each end of the transfer lines. The center (e) of the cell holds the desired detection volume. **B:** Actual image of a small volume cell with dried epoxy-glue plug, and fused-silica transfer lines. **C:** Single resonance circuit used in each coil with tuning capacitors, C_t (0–9 pF and 2.2 pF), matching capacitors, C_m (0–9 pF and 3.6 pF) and a 2 cm long, 0.181 in. OD, 50 Ω semi-rigid coaxial cable used to connect the coil to the rest of the circuit.

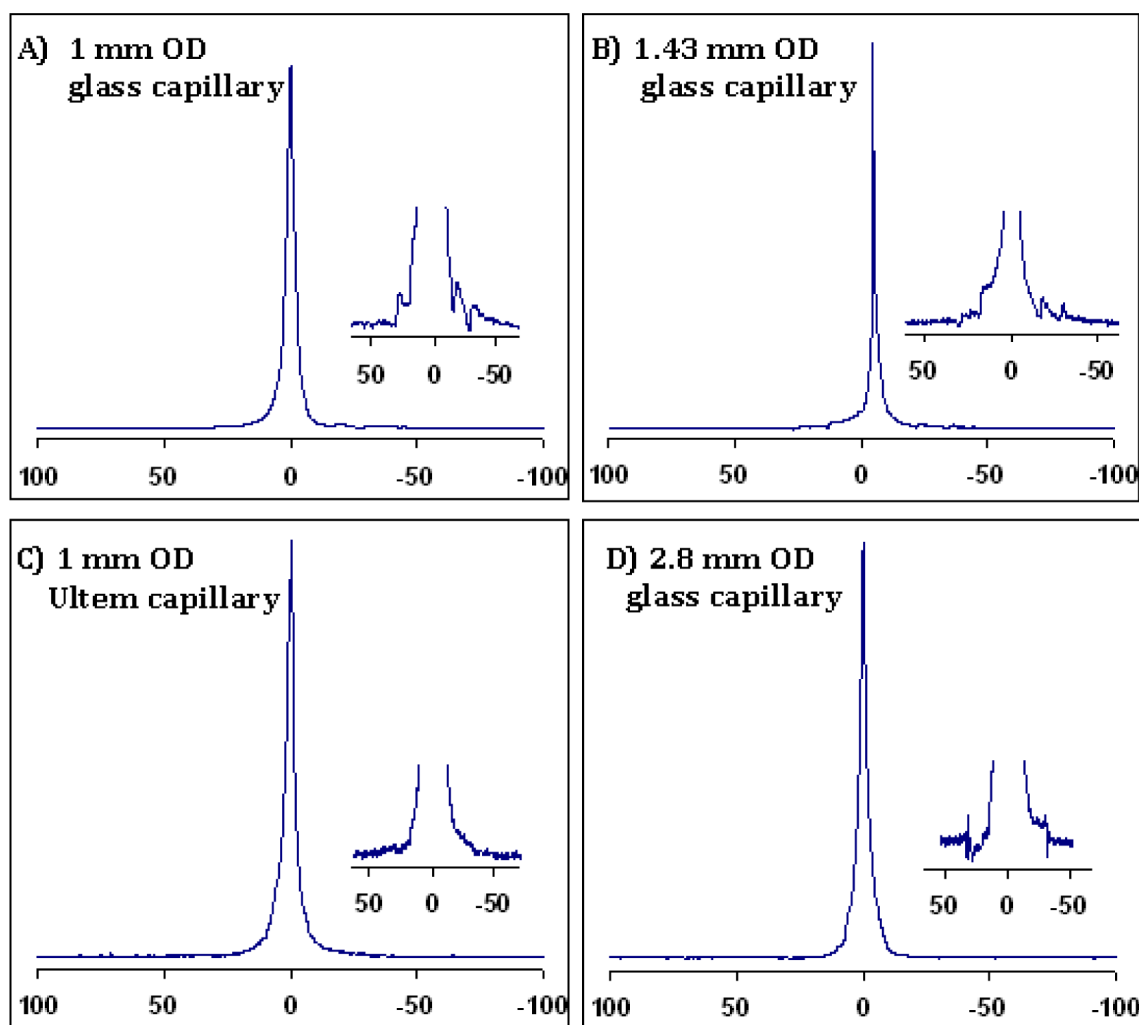


Fig. 3. ^1H spectra (in Hz) of 1% $\text{H}_2\text{O}/\text{D}_2\text{O}$ showing high resolution non-spin line shapes in small and large volume capillary cells with susceptibility-matched plugs. Insets show the baseline shapes close to 0.11% peak height. The best line shape is achieved using the 1 mm OD Ultem capillary (spectrum C) due to reduced susceptibility differences between the Ultem capillary, epoxy plug and surrounding fluorinert. (Resolution values are given in Table 1.)

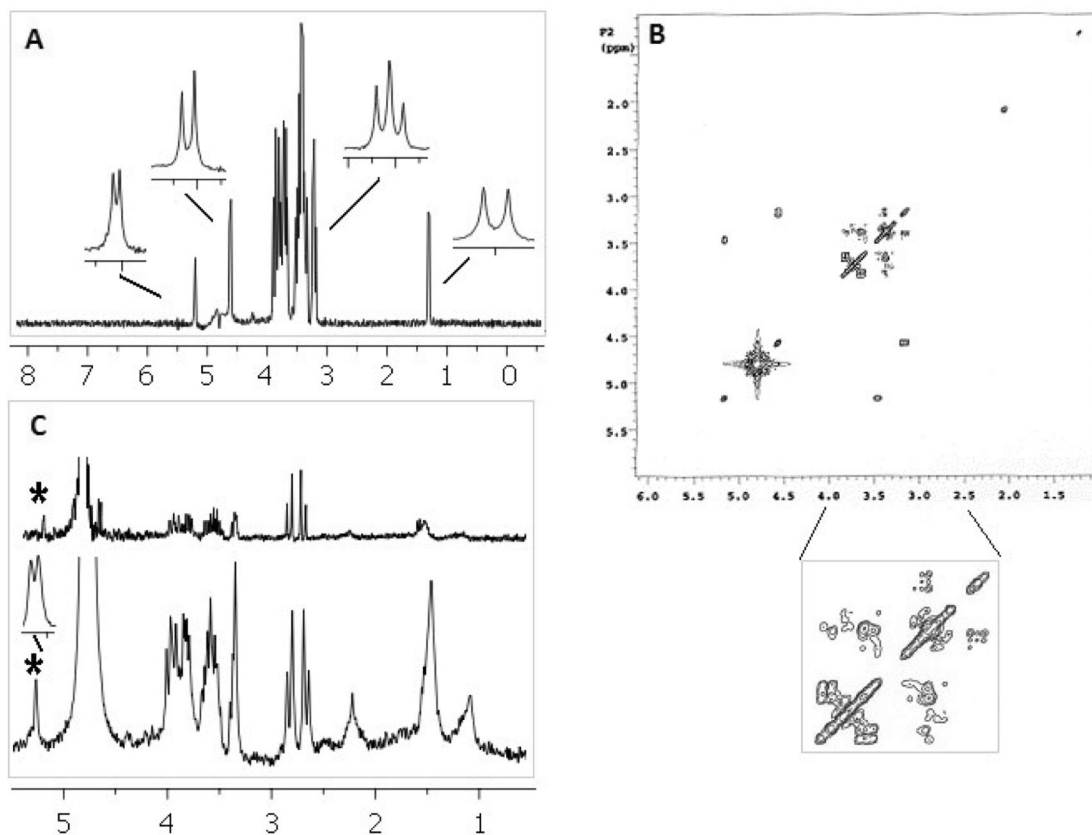


Fig. 4. High resolution 1D ¹H spectrum (A) and 2D COSY (B) of mixture (20 mM) of glucose and threonine acquired in 20- μ L coil with ulterm plugs. 1D insets show the resolved signature peak chemical shifts (glucose multiplets at 4.6, 5.2, and 3.2 ppm, and threonine doublet at 1.3 ppm). (C) 1D ¹H spectrum of deproteinated human plasma with 36 scans in the susceptibility plug containing 20- μ L probe (lower) and 5 mm conventional probe (upper). For the same mass of glucose raw SNR was 28.5:1 for a susceptibility plug microcoil probe compared to 3:1 for the 5 mm conventional probe.

Table 1
Comparison of small and larger volume microcoil sample cells with and without susceptibility-matching plugs

Cell type	*Total cell-sample volume		Volume Efficiency Enhancement	LW _{avg} 50/0.55/0.11 % peak ht.		Sensitivity _{avg} SNR 1% v/v H ₂ O/D ₂ O	
	Without Plugs	With Plugs		Without Plugs	With Plugs	Without Plugs	With Plugs
500 nL active volume (1.0 mm OD glass capillary)	9.5 μ L	0.8 μ L	11.9-fold	0.8/20/25 Hz	1.3/20/30 Hz (epoxy plug)	658	660
500 nL active volume (1.0 mm OD custom ultem capillary)	10 μ L	1.5 μ L	6.7-fold	1.2/34/44 Hz	1.5/38/48 Hz (epoxy plug)	660	662
2 μ L active volume (1.43 mm OD 1.05 mm ID glass capillary)	35 μ L	4 μ L	8.8-fold	0.8/28/31 Hz	0.9/36/40 Hz (epoxy plug)	950	940
20 μ L active volume (2.8 mm OD, 2.4 mm ID glass capillary)	140 μ L	24 μ L	6-fold (20–25 fold compared to 600 μ L, 5 mm NMR tube)	0.8/22/36	0.9/23/33 Hz (ultem plug)	3540	3530

* Transfer line volume (2.5 μ L for each of two 70 μ m ID, 55 cm long transfer lines) is not considered in the table above. SNR for a 4-nucleus Nalorac 5 mm probe for 1% v/v H₂O/D₂O was 4000 and 7800 with and without sample spinning, respectively.